Sensors and Materials, Vol. 31, No. 4 (2019) 1119–1134
MYU Tokyo

S & M 1839

Functionalization of a Diamond Surface through N_2 and H_2 Irradiation for Estrogen (17β-estradiol) Aptamer Sensing

Evi Suaebah,[1*] Masataka Hasegawa,[2] Jorge J. Buendia,[1] Wenxi Fei,[1]
Maneesh Chandran,[3] Alon Hoffman,[3] and Hiroshi Kawarada[1,4]

[1]Department of Nanoscience and Nanoengineering, School of Advanced Science and Engineering, Waseda University, Tokyo 169-8555, Japan
[2]Technology Research Association for Single Wall Carbon Nanotube (TASC), 1-1-1 Higashi, Tsukuba 305-8565, Japan
[3]Schulich Faculty of Chemistry, Technion-Israel Institute of Technology, Haifa 32000, Israel
[4]Kagami Memorial Research Institute for Material Science and Technology, Shinjuku-ku, Tokyo 169-0051, Japan

(Received December 4, 2018; accepted March 19, 2019)

Keywords: diamond, aptamer, surface, functionalization, estrogen

A label-free fluorescence aptasensor for the determination of 17β-estradiol (E2) was developed. The aptasensor was prepared by the functionalization of a diamond surface using a nitrogen radical beam (NRB) system to produce amine terminals on the diamond itself. The fabrication of the sensor was performed by photolithography to produce a dot pattern, which was used as a sensing area for activated biomolecules. The supporting DNA strands were immobilized and an aptamer was hybridized to prepare a detection pair to bind with any E2 molecule, as the aptamer captures the E2 molecule naturally. The fluorescence microscopy signal was used for the detection of E2. The biomolecule activities were determined through special treatment, with three different stages evident in the fluorescence result, namely, hybridization, detection, and denaturation. When E2 was detected by the aptamer, the intensity of the fluorescence signal decreased because of the aptamer binding with the E2 molecule. E2 was detected by determining the fluorescence signal intensity of the dot pattern. When the aptamer was released from the supporting DNA and formed a complex with the E2 molecule, the intensity of the dot pattern decreased rapidly. The difference between the two signals indicated the number of E2 molecules bound to the aptamer. The proposed method is simple and powerful for the detection of small molecules with high sensitivity by utilizing the basic reaction of aptamers.

1. Introduction

17β-estradiol, also known as E2, is a natural estrogen excreted by humans and animals, and has the greatest estrogenic activity.(1) E2 is one of the endocrine-disrupting steroid compound (EDC) hormones with a harmful effect on the endocrine function of the human body and

*Corresponding author: e-mail: evisuaebah@gmail.com
https://doi.org/10.18494/SAM.2019.2231

ISSN 0914-4935
https://myukk.org/

aquatic organisms, and one of the most encountered endocrine-disrupting molecules in the environment.[2,3] This natural steroid hormone, which plays an important role in reproduction and sexual function, has been found in the environment (in water) and human body.[4] It is an important diagnostic marker of various chemical conditions associated with sex hormone imbalance, such as puberty, fertility, ovarian tumor, prostate cancer, and breast cancer.[5] The rapid effect of E2 can cause several diseases as well as birth defects, development disorders in humans in low and high concentrations (natural and synthetic), and harmful effects in fish.[5,6] In this report, we demonstrate the detection of E2 by using an aptamer-based biosensor.

Recently, interest in the research on aptamers has rapidly increased.[7,8] Research into the application of aptamers to the sensing of small molecules has resulted in the development of advanced biosensors.[9–15] Aptamers are single-stranded DNA or RNA molecules with various shapes owing to their tendency observed in the systematic evolution of ligands by the exponential enrichment (SELEX) process.[16] Hence, they are extremely good for binding with a target with high affinity, selectivity, and specificity.[17–19] Common targets include proteins, peptides, carbohydrates, and small molecules.[20] The binding of aptamers is determined by their tertiary structure because they fit their targets from the SELEX process.[21] In addition, aptamers are more stable than antibodies and require less expensive purification steps.[22] E2 binds with the thymine loop region in the base pair aptamer part, which is common to all specific E2 aptamers in the literature.[23]

There has been considerable research interest in the preparation of sensors using diamonds with high sensitivity, and stability increases rapidly in both biological activation and surface functionalization.[24–26] Diamond is one of the most popular candidates as a biosensor material owing to its good electronic and chemical properties.[27–29] The surface functionalization of the diamond surface for sensing applications can be integrated into a single platform.[30,31] The most important properties of diamond are its excellent chemical stability and reusability.[12,32,33] Fluorescence sensing is the simplest and fastest method for the detection of small molecules using diamond as a sensing platform.[9,10] As an alternative, surface functionalization with an aptasensor has been explored for the detection of various small molecules and proteins.[34,35] Several biosensors for the detection of E2 have been deployed using E2 aptamers.[36–39] These biosensors can detect 17β-estradiol with good sensitivity (low concentration range of 2–5 nM). The sensitivity of each biosensor was evaluated at seven different E2 concentrations.

In this study, we functionalized a diamond surface with a short aptamer (35-mer) using a nitrogen radical beam (NRB) system to develop a biosensor for the detection of E2.[40–42] The aptamer was selected because it has high affinity and specificity to E2.[24] The biosensor was prepared by first immobilizing DNA (supporting DNA) onto a diamond surface.[43] Then, the fluorescence-labeled aptamer was introduced directly onto the supporting DNA to produce double-stranded DNA through hybridization. E2 was detected when the aptamer reacted with the E2 molecule and was released from the supporting DNA and formed a complex with the E2 molecule. The simplest thing that the aptamer followed naturally was binding with a target, which fits with its target.[43,44] The fluorescence signal indicated the sensing reaction for E2 detection.[45,46]

Amine termination allowed the covalent immobilization of the supporting DNA, which hybridized with aptamers to allow E2 detection. The resulting nanocrystalline diamond (NCD) with partial amine termination was expected to be stable after denaturation. In addition, fluorine termination was used to provide a nonspecific binding adsorption, which lowers the signal-to-noise ratio in the biosensor on a diamond surface. Fluorine termination is better than the use of oxygen or hydrogen as a passivation layer. The functionalization of the diamond surface can be used for various techniques and modifications. NV centers, high performance electricity, magnetic field, pressure, and temperature are considered in several techniques that can be used to understand a diamond surface with unique objects and a variety of applications. With this unique characteristic, we combine a diamond part with a biological part (DNA) as a sensing part for E2 detection.

We prepared a compact, simple, real-time, and easy-to-produce diamond sensor platform for the rapid, highly specific, and sensitive detection of E2.[40] Biosensor sensitivity, reusability, and specificity were evaluated in this study.

2. Experimental Methods

2.1 Reagents and materials

The estrogen aptamer (E2 aptamer) 5'-Cy5-AAG GGA TGC CGT TTG GGC CCA AGT TCG GCA TAG TG-3' was purchased from Alpha DNA (Quebec, Montreal, Canada) and the supporting DNA 5'-COOH- CA CTA TGC CGA ACT TGG GCC CAA ACG GCA TCC CTT-3' was purchased from Sigma-Aldrich (Tokyo, Japan). The molecule target aptamer, 17β-estradiol, was purchased from Sigma-Aldrich (Tokyo, Japan). A solution of phosphate-buffered saline (PBS; 1 mM NaCL, 2 mM NaH_2PO_4, 8 mM Ma_2HPO_4, 0.1% Tween-20) was prepared. The 3x sodium saline citrate (3x SSC), 0.1 M N-hydroxysuccinimide (NHS), and 0.4 M ethyl-3-(3-dimethylaminopropyl) carbodiimide hydrochloride (EDC) were mixed at a ratio of 2:1:1 for the dilution of the supporting DNA before immobilization (activation treatment). Tris-EDTA (TE; 10 mM Tris-HCL, 1 mM EDTA, pH 8.0) buffer solution was prepared for washing. All reagents used were of analytical grade. Ultrapure water was used as a washing solution for the reactions.

2.2 Apparatus

The fluorescence signal detection system consisted of a fluorescence microscope (Olympus 1X71; Olympus, Tokyo, Japan). A dot pattern on the diamond surface was employed throughout the experiment. The dots formed an active area containing amine terminals, which naturally reacted with the supporting DNA and became the sensing detection area. The dot patterns on the diamond surface became luminescent when the aptamer and supporting DNA hybridized. The luminescence of the double strand resulted from the fluorescent dye (Cy5), which was directly attached to the aptamer.

2.3 Fabrication of the aptasensor

Prior to modification, the diamond surface was modified with a NRB system. The NCD substrate was treated with a strong acid to produce the starting surface containing oxygen terminals. The partial oxygen termination was conducted a second time using an ultraviolet light (UV) ozone cleaner for 2 h at room temperature (RT). The partial oxidation of the diamond surface was performed using a low-pressure mercury lamp that emits UV with a wavelength of 257.3 nm. Nitrogen gas was introduced into the reaction chamber for 5 min to purge the gases inside the chamber; oxygen gas was then introduced for less than 10 min, and the substrate was irradiated with UV light for 2 h. This process resulted in the growth of strong oxygen terminals on the diamond surface. The oxygen-terminated surface interacted well with nitrogen radicals to form a nitrogen-terminated surface. Irradiation with nitrogen radicals was carried out in a vacuum chamber for 20 min at 200 °C. Prior to nitrogen radical exposure, N_2(96%)/H_2(4%) gas was introduced into the chamber for 10–20 min before the start of radical treatment and the temperature was increased to 200 °C. The N_2/H_2 gas was allowed to flow for approximately 10 min after the radical treatment.

The diamond surface was fabricated by photolithography using a gold mask as an initial mask for dot fabrication. Gold was deposited on the diamond surface with a thickness of approximately 150 nm. The micropattern formed on the diamond surface is vital for separating the diamond area to allow for distinctive functionalization, that is, amine functionalization inside the uniform dot and a fluorinated component outside the dot. The resulting micropattern had a hydrophilic surface inside the feature where the functionalized group still remained and a hydrophobic surface in the region was terminated with fluorine, enabling the easy filling of the micropattern with an aqueous solution containing the biomolecules of interest. To induce chemical reactivity, the amine groups were activated with EDC NHS solution for 30 min.

2.4 Assay of aptasensor

The detection and quantification of E2 were performed by adding the supporting DNA to bind with the aptamer and immobilizing it on the diamond surface. The aptamer was modified with a fluorescent dye on the 5'-end and hybridized with the supporting DNA. The DNA aptamer and its complementary DNA (supporting DNA immobilized on diamond) were used as the E2 detector. This supporting DNA was immobilized on the partially aminated diamond surface through covalent bonding. The immobilization probe DNA was 20 μm supporting DNA, +3x sodium saline citrate (SSC) buffer solution, 0.1 M N-hydroxysuccinimide (NHS), and 0.4 M ethyl-3-(3-dimethylaminopropyl) carbodiimide hydrochloride (EDC) mixed solution in a ratio of 2:1:1. The sample was incubated for 2 h in a humidified chamber at 38 °C. After the immobilization, the immobilized DNA was washed with PBS for 5 min and then with deionized water for 2 × 5 min to remove the physically absorbed material from the diamond surface. In the case of E2, the concentration of the E2 aptamer solution was 10 μM in TE buffer and the aptamer was incubated in the humidified chamber at 25 °C for 1 h. The aptamer hybridized

with the supporting DNA. The aptamer was washed with a buffer solution at RT for 5 min and then with deionized water for 2 × 5 min.

The first fluorescence signal was observed using an epifluorescence microscope (Olympus 1X71; Olympus, Tokyo, Japan) as a hybridization process. The E2 target solution was diluted with 2x SSC and incubated at RT for 1 h. Subsequently, the sample was rinsed with TE buffer for 5 min and deionized water for 2 × 5 min. A schematic illustration of the E2 detection procedure of the aptamer is shown in Fig. 1.

E2 was detected by the natural binding affinity of the aptamer. The thymine-rich part of the aptamer locked with the E2 molecule and the single-stranded DNA of the aptamer, and formed a loop with the E2 molecule in one part. The biomolecule activation scheme is shown in Fig. 1.

The supporting DNA was immobilized on the diamond surface directly through covalent bonding between the amine-terminated diamond surface and the carboxyl groups on the supporting DNA. The aptamer was directly dropped onto the diamond surface and immobilized by the supporting DNA. The hybridization occurred naturally between the supporting DNA and the aptamer to form a double strand, with the fluorophore-modified dye on the aptamer 5'-end, which interacted with the microscope and showed a change in signal intensity from low to high. When the E2 target was released to the diamond surface, the aptamer naturally became active and was released from the supporting DNA. The aptamer formed a complex with the E2 target and was released from the supporting DNA. During this process, the fluorescence signal intensity decreased immediately. The final stage of the biomolecule activity was denaturation. Denaturation removed all physical binding components and left only the supporting DNA on the diamond surface.

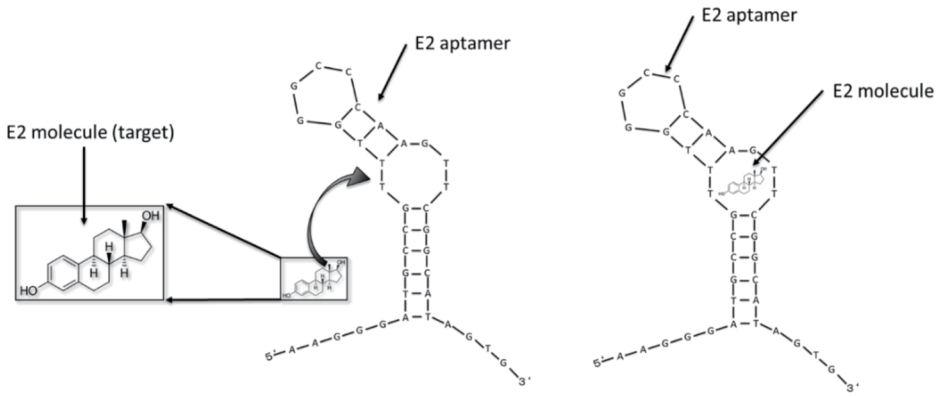

(a) (b)

Fig. 1. Structure of the 35-mer E2 aptamer and E2 molecule. Schematic illustration of the aptamer sensing process for E2 detection by the aptamer. (a) E2 molecule (inset) as a target molecule for the E2 aptamer (not actual size). (b) The aptamer naturally forms a complex with the E2 molecule in the thymine-rich part.

3. Results and Discussion

3.1 X-ray photoelectron spectroscopy (XPS) measurement of the amine termination by NRB system

The surface functionalization treatment by NRB was observed by XPS and HREELS to characterize the diamond film. Figure 2 shows the wide survey spectra of diamond after NRB treatment. Beside the C1S core level peaks, the surface spectra of the diamond surface also showed another strong peak at approximately 399.39 eV, which was attributed to nitrogen functionalization induced by the NRB system. The high intensity of the nitrogen peak indicated a high coverage of nitrogen, but not only of the aminated area on the diamond surface. The use of the NRB system is an effective and simple method because it does not require the use of wet chemical techniques to functionalize a diamond surface. The irradiation technique together with N_2/H_2 gas can induce amide bonding on the diamond surface.

The surface component was analyzed by XPS, and N–H bonding was observed by HREELS. The density of each carbon-bonding-related functionalization was calculated by taking the percentage of the peak area. Every single bonding was represented by an area and indicated by monolayer calculations. However, the percentages of various lines of carbon-related chemical functionalization were determined in the same manner. The nitrogen termination was 0.5 ML thickness. This indicated that approximately 50% of the N_2/H_2 termination on the diamond layer was covered by nitrogen and transformed to amine termination. This amine termination actively occurred during interaction with complex molecules such as DNA, RNA, or even other biomolecules for activation. As shown in Fig. 2(b), after irradiation with N_2/H_2 gas at 200 °C, N–H bonding was clearly evident at 420 meV. HREELS measurement was performed

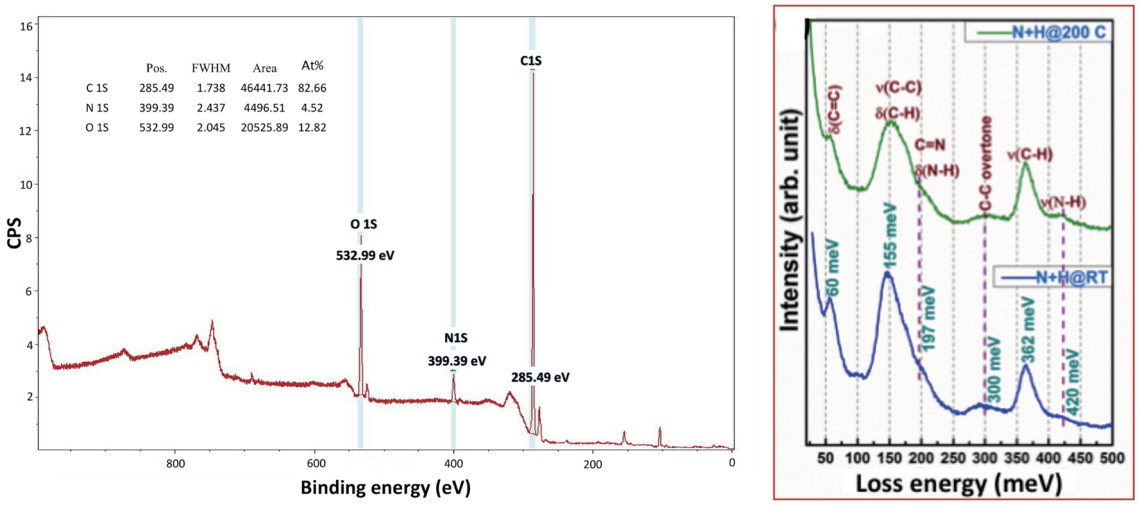

(a) (b)

Fig. 2. (Color online) (a) XPS spectrum of the nitrated diamond surface by NRB formed for 20 min. The N1S peak was detected at 399.39 eV. (b) High-resolution electron energy loss spectroscopy (HREELS) spectra of NCD after NRB treatment for 20 min at 200 °C and RT.

after the annealing at 250 °C to remove the adsorbed water/ambient contaminants. The sample prepared at 200 °C clearly displayed an N–H stretching mode. The relatively high intensity N–H stretching mode observed in the sample prepared at Technion using RF N_2 plasma may be due to the presence of a high concentration of nitrogen (~15 at.%).[47]

Direct amination in the NRB system is supposed to terminate in the high amine region of the diamond surface. C–H, COOH, or C–OH reacted with N_2/H_2 gas and the continuous irradiation by plasma at a low power for 20 min resulted in the formation of C–NH_2 on the diamond surface. However, strict limitation will limit the amine group coverage on the surface to a certain level. The C1S peak from diamond was detected at the usual carbon peak position at 284.4 eV. The corresponding ratio of the nitrogen peak was ~4% in addition to the existence of nitrogen (amine), which was confirmed by the N1S peak after amination.

3.2 Immobilization of supporting DNA on the sensor surface

The supporting DNA was a single-stranded DNA without a fluorescence label. The 5'-end was modified with a carboxyl compound to induce bonding between the surface and the biomolecules. The covalent bonding of the supporting DNA through the carboxyl and amine groups on the diamond surface was achieved naturally. To evaluate the immobilization result and confirm that the observed fluorescence signal was due to the formation of an amine linker, we conducted several washing treatments after hybridization.

When the supporting DNA was directly attached onto the diamond surface, the NRB process was necessary for the formation of the amine compound. The gas flow before the irradiation treatment had a critical effect. Immobilization occurred when covalent bonds were formed between the aminated diamond surface and the COOH of the single-stranded DNA. In addition, amine termination was activated by the EDC:NHS solution for 45 min. Activated amine bonding ensures that amine and COOH from DNA can bond perfectly. The strong bonding between the diamond and the DNA was unbreakable. This was an important step for the use of activated diamond as an aptasensor. When the diamond surface did not contain amines, the immobilization of the single-stranded DNA through covalent bonding was impossible. Therefore, amine termination was important for further surface functionalization. The NRB technique is the newest technique for the functionalization of diamond through amine bonding. It is a simple and unique technique for obtaining amine-terminated diamond surfaces.

The diamond functionalization technique requires a purging gas pipe before and after the irradiation treatment. Amine bonds are easier to produce on the diamond surface when N_2/H_2 is free from other gas contaminants. The primary amine groups from the N_2/H_2 purging gas are attractive starting points for further modification of the diamond surface. N_2 and H_2 as purging gases directly attach to diamond (physisorption) as precursors of amine termination, and then by irradiation, they are decomposed to form amine termination on the diamond surface. This technique for the functionalization of a diamond surface is an attractive starting point for the attachment of complex molecules such as DNA, RNA, or even cells for biosensing applications. When only an irradiation gas was applied to the diamond surface without purging, hybridization did not occur after 1 h incubation and washing treatment. This indicated that no immobilization occurred between the supporting DNA and the diamond surface. If the immobilization does not

occur on the diamond surface, hybridization will also be impossible. Therefore, the covalent bonding between the supporting DNA and the diamond surface, as well as hybridization, did not occur. To determine the strength of hybridization on the diamond surface, washing treatment was used as an alternative method to determine the success of hybridization on the diamond surface.

Hybridization was achieved between the supporting DNA and the fluorescence-labeled aptamer. As shown in Fig. 3(a), the first fluorescence signal was observed when good hybridization occurred between the supporting DNA and the aptamer. The high fluorescence signal intensity originating from hybridization in the dot pattern shows a great image with high intensity. When the washing treatment was applied to the diamond surface [Fig. 3(b)], the intensity of the dot pattern decreased. The average thickness of N is 0.9 ML.[48] This means that the diamond surface was uniformly covered by N. From the N density on the diamond surface, the maximum nitrogen coverage was estimated to be about 90% from the XPS data. From this value, a high percentage of amine is expected to be immobilized with the supporting DNA, and aptamer hybridization is considered to depend on the density and concentration of the supporting DNA. This result shows that the physical bonding between the diamond and the aptamer was inhibited by the washing treatment. As shown in Figs. 3(a) and 3(b), the intensity of the fluorescence signal of hybridization between the aptamer and the supporting DNA was highly stable and not disturbed by the washing treatment.

3.3 Aptasensor for E2 detection

The selectivity and sensitivity of an aptamer are key criteria for biosensing applications and display several advantages. The E2 aptamer was selected by an *in vitro* process to produce the binding ability with the E2 molecule. The supporting DNA immobilized on the amine group on the diamond surface was accessible to specific hybridization with the E2 aptamer. The hybridization of the aptamer was a one-step technique for E2 detection using fluorescence. The

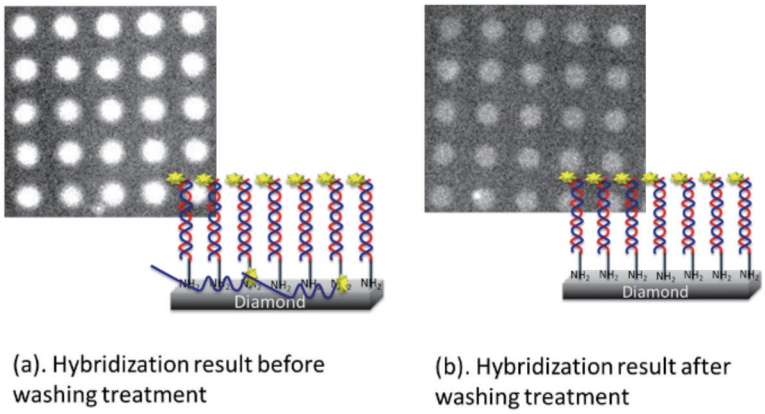

Fig. 3. (Color online) The real binding is not affected by washing treatment. (a) Physical binding conducted when aptamer hybridized with supporting DNA. (b) The washing process removed the physical bonding between the aptamer and the diamond.

epifluorescence microscopy image of the cyanine5 (Cy5)-labeled fluorophore aptamer coupled with the supporting DNA was obtained on a circular micropattern of 20 μm diameter of the amine-rich area on the diamond surface.

The hybridization characteristics of the aptamer and supporting DNA are shown as fluorescence microscopy results. After incubation for 1 h at 25 °C, washing treatments were performed to verify and inhibit the nonspecific and physical bonding processes on the diamond surface. Only covalently bonded molecules with high stability remained on the diamond surface.[9,10]

The intensity of the circles on the diamond surface increased with the length of hybridization. First, the fluorescence signal occurred during hybridization. No fluorescence signal was evident after the initial immobilization step. The successful bonding between the amine and the supporting DNA resulted in the bonding between the supporting DNA and the aptamer through hybridization. During hybridization, the fluorescence signal increased directly with high intensity.

In this aptasensor, the fluorescence intensity depended on the conformational change of the aptamer and E2 target. During hybridization, the dot patterns were formed with high intensity and clearly showed a different signal between the amine-rich area and the background area covered by fluorine.

The change in fluorescence intensity due to a conformational change occurred when the E2 molecule was introduced to the diamond surface and bound to the aptamer. E2 became the aptamer target and formed a complex with the aptamer. The natural bonding between the aptamer and the E2 molecule depended on the aptamer characteristic itself. The aptamer bonding only fit with one kind of target. The structure of the aptamer and E2 molecule is shown in Fig. 1.

The binding between the aptamer and the E2 molecule altered the fluorescence intensity of the dot pattern. The fluorescence intensity decreased as the E2 molecule took the place of the aptamer. Thus, the change in fluorescence intensity could be used for sensing detection using a diamond aptasensor. The fluorescence signal characteristics of the diamond indicated that the E2 molecule attracted the fluorescence intensity on the diamond surface.

The reduction in fluorescence intensity was due to the aptamer/target binding ability, which was caused by the release of the aptamer from the supporting DNA. The aptamer formed a complex with E2. Specific binding occurred in the central stem loop region with the minimum energy.[2] E2 bound to the loop formed by thymines (T-loop). A similar T-loop is presented in the circle where the E2 molecule forms a complex with the aptamer.[3,4]

The E2 molecule is small and thus is difficult to detect compared with the protein target. The detection of small molecules is challenging, and until now, the small molecules that have been used are ATP, BPA, theophylline, tetracycline, and ampicillin (using DNA and RNA aptamers).[49–51] The E2 detection process is shown in Fig. 4. The following are the three biomolecular activities steps observed to occur on the diamond surface: hybridization, detection, and denaturation.

Figure 4 shows how the aptamer detection process can be used as a strategy for E2 detection: (a) The covalent bonding between the supporting DNA and the aptamer occurred at the initial

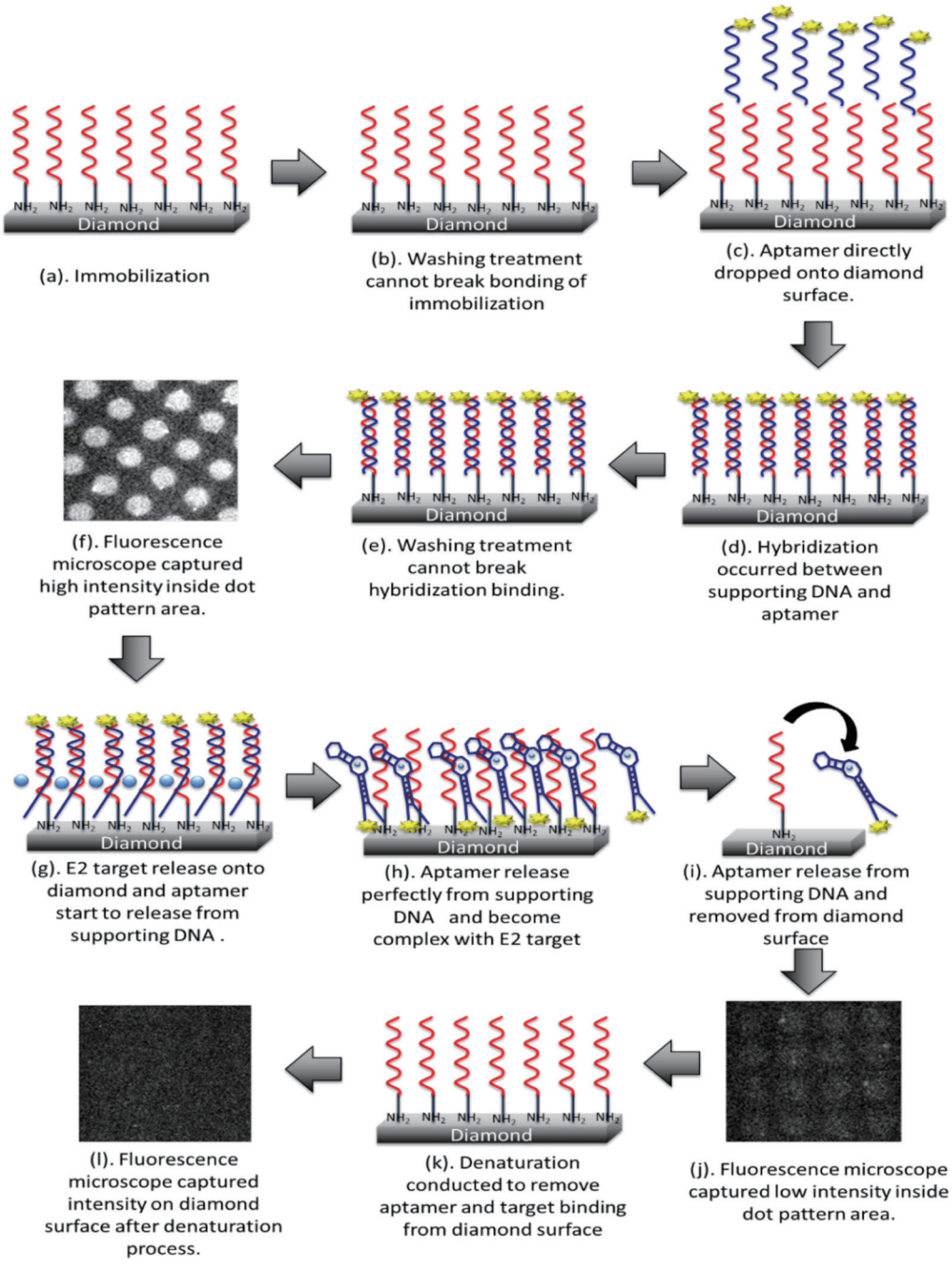

Fig. 4. (Color online) Aptamer detection process. (a) Immobilization conducted between diamond and supporting DNA, (b) washing treatment conducted to inhibit physical binding on the diamond surface, (c) aptamer directly dropped on the diamond surface, (d) hybridization occurred between the aptamer and the supporting DNA to form a double strand, (e) washing treatment conducted to inhibit physical binding between aptamer and diamond, (f) high-intensity fluorescence microscopy image of the dot pattern, which shows that hybridization was successful, (g) E2 target dropped on the diamond surface and the aptamer started to be released from the supporting DNA, (h) the E2 target was captured by aptamer, which departed from the supporting DNA and formed a complex with the aptamer, (i) illustration of aptamer forming a complex with the E2 target, (j) low-intensity fluorescence microscopy image after E2 detection, (k) denaturation was performed to inhibit the physical binding on the diamond surface, and (l) fluorescence microscopy image without the dot pattern.

stage, (b) a washing treatment was performed to inhibit nonspecific and physical binding processes on the diamond surface, and the covalent bonding between the diamond surface and the supporting DNA during immobilization was not broken by washing. The natural binding between the supporting DNA and the aptamer [Figs. 4(c) and 4(d)] indicated hybridization and was used as the initial stage for capturing the first fluorescence signal with the microscope. The fluorescence signal indicated the successful hybridization between the supporting DNA and the aptamer [Figs. 4(e) and 4(f)]. The highest fluorescence signal intensity was observed immediately after hybridization when the aptamer formed a double strand with the supporting DNA and the Cy5 dye was activated using the fluorescence microscope. The density of the aptamer was controlled by varying the concentration of the supporting DNA during immobilization and the aptamer concentration during hybridization. When E2 was released to the diamond surface [Figs. 4(g)–4(i)], the aptamer formed a complex with the target and came off the supporting DNA. The supporting DNA became a single strand on the diamond surface and the E2 molecule target bound to the thymine loop of the aptamer. The stability of the double-stranded bonding was destroyed by the E2 molecule target, and the aptamer showed specificity and could detect the special target. A reduction in fluorescence signal intensity occurred at this stage and was recognized as the sensing of E2 [Fig. 4(j)]. Figures 4(k) and 4(l) show the denaturation process when the aptamer was released from the supporting DNA and remained on the diamond surface. The diamond surface could be modified by another hybridization process to form a new surface for the detection of the E2 aptamer. The reusability of the sensor was investigated. The results showed that the sensor is a good candidate for long-term storage.[10] The sensing between the aptamer and the E2 molecule on the diamond surface was conducted when the E2 molecule was detected by the aptamer and removed from the supporting DNA on the diamond surface. The fluorescence signal intensity showed that the E2 molecule was detected by the aptamer.

The fluorescence signal intensity was calculated on the basis of the extent of hybridization and E2 detection. From Fig. 5, the average intensity of the E2 target detection decreased to approximately 70%. This result confirmed that the binding of the aptamer to the E2 molecule was successful, i.e., approximately 70% of the total binding. The rest of the aptamer still remained on the diamond surface. Double-strand bonding results in the high stability of the aptamer. Hybridization occurred when the aptamer remained on the diamond surface. In this situation, the highest fluorescence signal intensity was observed. The modification of the aptamer with the Cy5 dye indicated a successful hybridization. The detection characteristic of the target was followed by aptamer E2 binding, which is presented by the fluorescence signal intensity.

The double-stranded DNA can be decomposed to form single-stranded DNA molecules not only during detection, but also during denaturation. Denaturation was used to remove all the biomolecules from the supporting DNA. This process left only the supporting DNA on the diamond surface.

The hybridization between the supporting DNA and the aptamer occurred when two DNA strands were held together by hydrogen bonding. The hydrogen bond on a double helix can be decomposed by an energy source. The aptamer itself becomes a lock and key with its target.

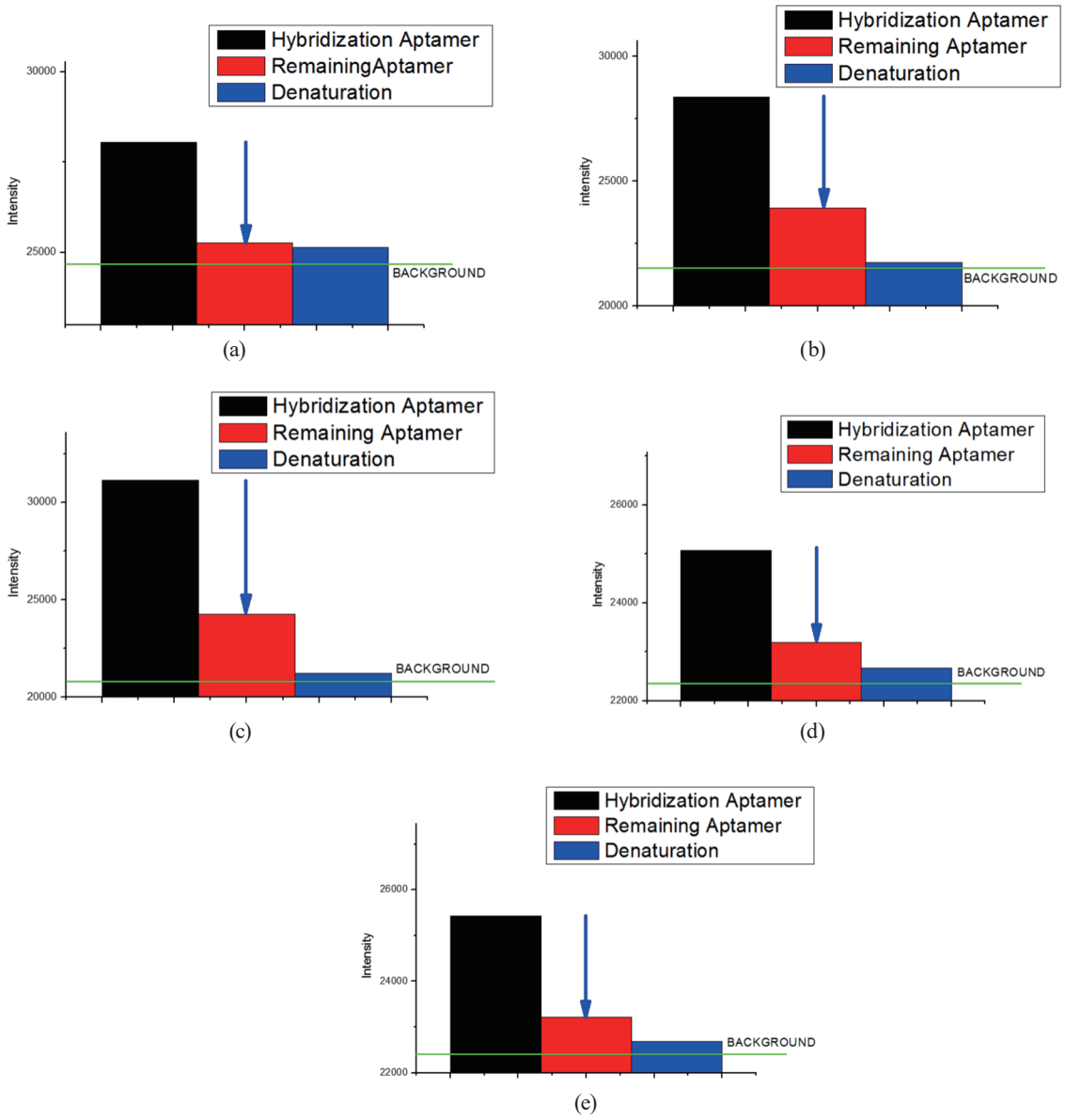

Fig. 5. (Color online) Comparison of the relative fluorescence signal intensity at three observation stages (hybridization aptamer, remaining aptamer on the surface after E2 attracted aptamers, and denaturation) of the biomolecule activities on the diamond surface conducted in five different samples. (a) Fluorescence signal intensity at three observation stages in sample 1, (b) fluorescence signal intensity at three observation stages in sample 2, (c) fluorescence signal intensity at three observation stages in sample 3, (d) fluorescence signal intensity at three observation stages in sample 4, and (e) fluorescence signal intensity at three observation stages in sample 5.

When the target is dropped on the diamond surface, a new source of energy can decompose the double helix formed during DNA hybridization and form a complex with the aptamer. The aptamer has a standard mechanism opposite to that of nucleic acid. Oligonucleotides are often represented as a linear sequence, but in reality, they fold into a specific conformation. The SELEX process allows the simultaneous screening of 1×10^{15} oligonucleotides against a target of interest such as E2 in this case.

In our case, when the double-stranded DNA attracts the E2 molecule, the stability of the double strand is immediately disturbed. The aptamer is instantly released from the supporting DNA and becomes active in detecting the E2 target. When the aptamer is released completely from the supporting DNA, the E2 target naturally forms a complex with the aptamer in the loop region as a lock and key. In this aptamer, thymines are active parts that bind with the E2 molecule target. In the SELEX process, a DNA folding becomes a loop or a hairpin depending on the target characteristic, and the DNA that interacts with the target through a statistical process in a huge chamber is reduced into small pieces.

3.4 Reusability

Reusability studies were performed to determine the capability of using the diamond surface for multiple sensing applications. After denaturation, the diamond surface could be renaturated (rehybridized with the aptamer for sensing activities). Figure 6 shows the reusability of the diamond sensor for aptamer detection.

E2 detection was repeated three times. The diamond modified with amine terminals is a good candidate for frequent reuse. As shown in Fig. 6, the aptasensor could be reused for the coupling of the aptamer with the supporting DNA. The stability of the sensor was indicated by the fluorescence signal in the hybridization step. The fluorescence signal following hybridization was stable after the aptasensor was reused three times in different samples [Figs. 6(a) and 6(b)]. This confirmed that the NCD-based aptasensor is reusable for long-term use. The Comparison of Figs. 5 and 6 shows the stability of the biosensor after several uses. As shown in Fig. 5, data were collected from several samples to show that the fluorescence signal intensity is similar in several samples.

As shown in Fig. 7, E2 detection was conducted from high to small E2 concentrations. We measured the lowest E2 concentration at 0.1 μM, indicating a successful E2 detection at a low E2 concentration.

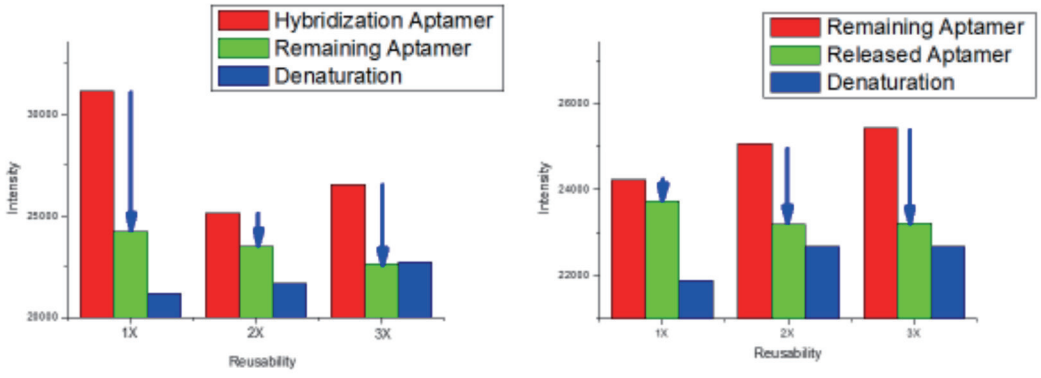

(a) (b)

Fig. 6. (Color online) Reusability of diamond sensor for E2 detection in different samples. Samples have the same characteristic and treatment. (a) Reusability result from sample 1 and (b) reusability result from sample 2.

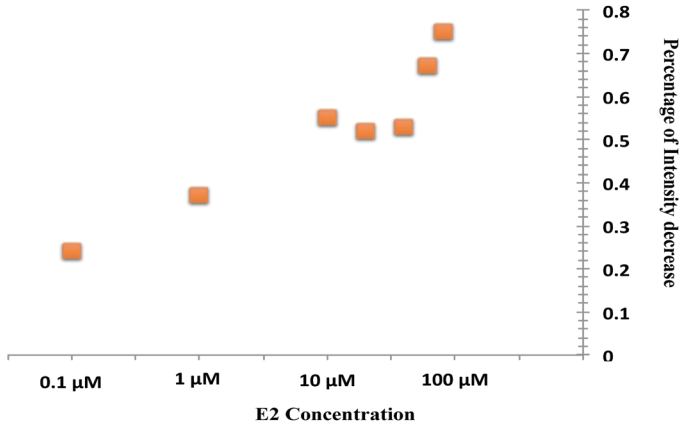

Fig. 7. (Color online) Variant of E2 concentration obtained by aptamer detection through decrease in intensity.

4. Conclusion

The corresponding ratio of the nitrogen peak was ~4% in addition to the existence of nitrogen (amine), which was confirmed by the N1S peak after amination. The stability of the sensor is indicated by the fluorescence signal after the hybridization step. The fluorescence signal following hybridization was stable even after the aptasensor was reused seven times. The dot pattern remained on the diamond surface after seven cycles, indicating that detection by the aptamer was still possible. This confirmed that the NCD-based aptasensor is reusable.

The immobilization of the supporting DNA was successfully achieved using a nitrogen and hydrogen radical beam system. The strong bonding between diamond and DNA was unbreakable. Leakage gases before irradiation treatments improved amine termination on the diamond surface. Without a leakage gas, amine termination was not terminated successfully. The estrogen hormone is a small molecule, which is found in the human body and environment. E2 detection is difficult because of the size of the molecule compared with that of the protein. The successful detection of E2 by an aptamer on a diamond surface is promising for the development of biosensing platforms with high performance.

The detection of E2 at various concentrations showed that the activity of the aptamer was acceptable and had good performance on the diamond substrate. The lowest E2 concentration that could be detected was 0.1 µM, which is sufficient for biosensing application. Amine termination is a chemical modification that can be used for complex applications and modifications of surfaces with biological substrates. The simplest modification was achieved successfully with high performance.

Acknowledgments

This work was supported by a Grant-in-Aid for GCOE Research from the Ministry of Education, Culture, Sports, Science and Technology. E. Suaebah gratefully acknowledges the Ministry of Directorate of General Higher Education Indonesia (DGHE/DIKTI) for a scholarship award.

References

1 G. G. Ying, R. S. Kookana, and Y. J. Ru: Environ. Int. **28** (2002) 545. https://doi.org/10.1016/S0160-4120(02)00075-2
2 M. Sun, L. Du, S. Gao, Y. Bao, and S. Wang: Steroids **75** (2010) 400. https://doi.org/10.1016/j.steroids.2010.02.002
3 H. B. Wei, J. M. Lin, D. N. Wu, L. X. Zhao, Z. J. Li, and X. T. Ying: Chin. J. Anal. Chem. **35** (2007) 319. https://doi.org/10.1016/S1872-2040(07)60037-1
4 V. Belgiorno, L. Rizzo, D. Fatta, C. D. Rocca, G. Lofrano, A. Nikolaou, V. Naddeo, and S. Meric: Desalination **215** (2007) 166. https://doi.org/10.1016/j.desal.2006.10.035
5 H. Kuramitz, M. Matsuda, J. H. Thomas, K. Sugawarac, and S. Tanaka: Analyst **128** (2003) 182.
6 H. S. Chang, K. H. Choo, B. Lee, and S. J. Choi: J. Hazard. Mater. **172** (2009) 1. https://doi.org/10.1016/j.jhazmat.2009.06.135
7 H. Y. Kong and J. Byun: Biomol. Ther. **21** (2013) 423. https://doi.org/10.4062/biomolther.2013.085
8 R. E. Wang, Y. Zhang, J. Cai, W. Cai, and T. Gao: NIH Public Access **18** (2011) 4175.
9 E. Suaebah, T. Naramura, M. Myodo, M. Hasegawa, S. Shoji, J. J. Buendia, and H. Kawarada: Sensors **17** (2017). https://doi.org/10.3390/s17071686
10 E. Suaebah, Y. Seshimo, M. Shibata, S. Kono, M. Hasegawa, and H. Kawarada: J. Appl. Phys. **121** (2017) 44506. https://doi.org/10.1063/1.4974984.
11 E. Suaebah, T. Naramura, and H. Kawarada: 2015 IEEE Sensors (IEEE, 2015) 15717372. https://doi.org/10.1109/ICSENS.2015.7370587
12 W. Yang, O. Auciello, J. E. Butler, W. Cai, J. A. Carlisle, J. E. Gerbi, D. M. Gruen, T. Knickerboker, T. L. Lasseter, J. N. Russell, L. M. Smith, and R. J. Hammers: Nat. Mater. **1** (2002) 253. https://doi.org/10.1038/nmat779
13 H. Kaur, J. G. Bruno, A. Kumar, and T. K. Sharma: Theranostics **8** (2018) 4016. https://doi.org/10.7150/thno.25958.
14 A. Ruscito and M. C. Derosa: Front. Chem. **4** (2016) 14. https://doi.org/10.3389/fchem.2016.00014
15 M. A. D. Neves, S. Slavkovic, O. Reinsteins, A. A. Shoara, and P. E. Johnson: RSC Adv. **9** (2019) 1690. https://doi.org/10.1039/C8RA07462C
16 A. D. Ellington and J. W. Szostak: Nature **355** (1992) 850. https://doi.org/10.1038/355850a0
17 B. Zhu, O. A. Alsager, S. Kumar, J. M. Hodgkiss, and J. Travas-Sejdic: Biosens. Bioelectron. **70** (2015) 398. https://doi.org/10.1016/j.bios.2015.03.050
18 J. J. Zhang, J. T. Cao, G. F. Shi, K. J. Huang, Y. M. Liu, and Y. H. Chen: Anal. Methods **6** (2014) 6796. https://doi.org/10.1039/C4AY01147C
19 H. Hasegawa, N. Savory, K. Abe, and K. Ikebukuro: Molecules **21** (2016) 421. https://doi.org/10.3390/molecules21040421
20 V. Vemeeren, S. Wenmackers, M. Daenen, K. Haenen, and P. Wagner: Langmuir **24** (2008) 9125. https://doi.org/10.1021/la800946v
21 S. U. Akki, C. J. Werth, and S. K. Silverman: Natural Waters **49** (2015) 9905. https://doi.org/10.1021/acs.est.5b02401
22 R. E. Wang, H. Wu, Y. Niu, and J. Cai: Curr. Med. Chem. **8** (2011) 27 https://doi.org/10.2174/092986711797189565
23 G. S. Baird: Am. J. Clin. Pathol. **134** (2010) 529.
24 T. A. Hilder and J. M. Hodgkiss: Chem. Phys. Chem. **18** (2017) 1881. https://doi.org/10.1002/cphc.201700363
25 L. C. Lora Huang and H. C. Chang: Langmuir **20** (2004) 5879. https://doi.org/10.1021/la0495736
26 T. Knickerbocker, T. Strother, M. P. Schwartz, J. N. Russell, J. Butler, L. M. Smith, and R. J. Hamers: Langmuir **19** (2003) 1938. https://doi.org/10.1021/la026279+
27 S. Szunerits and R. Boukherroub: J. Solid State Electron. Chem. **12** (2008) 1205. https://doi.org/10.1007/s10008-007-0473-3
28 J. T. Paci, H. B. Man, B. Saha, D. Ho, and G. C. Schatz: J. Phys. Chem. **117** (2013) 17256. https://doi.org/10.1021/jp404311a
29 J. H. Yang, K. S. Song, G. J. Zhang, M. Degawa, Y. Sasaki, I. Ohdomori, and H. Kawarada: Langmuir **22** (2006) 11245. https://doi.org/10.1021/la0606771
30 C. E. Nebel and J. Ristein: Thin-Film Diamond I. Semiconductors and Semimetals (Elsevier Academic Press, Amsterdam, 2003).
31 V. N. Mochalin, O. Shenderova, D. Ho, and Y. Gogotsi: Nat. Nanotechnol. **7** (2011) 11.
32 M. H. Nazare and A. J. Neves: EMIS Data Review Series No. 26 (INSPEC Publication, 2001).
33 C. E. Nebel, B. Rezek, and D. Shin: J. Phys. D: Appl. Phys. **40** (2007) 6443.
34 J. He, G. Li, and Y. Hu: Anal. Chem. **87** (2015) 11039. https://doi.org/10.1021/acs.analchem.5b03049

35 C. P. Gonzalez, D. A. Lafontaine, and J. C. Penedo: Front. Chem. **4** (2016) 1. https://doi.org/10.3389/fchem.2016.00033
36 N. Yildirim, F. Long, C. Gao, and A. Z. G: Environ. Sci. Technol. **46** (2012) 3288. https://doi.org/10.1021/es203624w
37 S. G. Kim, J. S. Lee, J. Jun, D. H. Shin, and J. Jang: ACS Appl. Mater. Interfaces **8** (2016) 6602.
38 H. Y. Zheng, O. A. Alsager, C. S. Wood, J. M. Hodgkiss, and N. O. V. Plank: J. Vac. Sci. Technol, B **33** (2015) 06F904
39 C. Chen, B. Liang, D. Lu, A. Ogino, X. Wang, and M. Nagatsu: Carbon **48** (2010) 939. https://doi.org/10.1016/j.carbon.2009.10.033
40 O. A. Alsager, S. Kumar, B. Zhu, J. T. Sejdic, K. P. McNatty, and J. M. Hodgkiss: Anal. Chem. **87** (2015) 4201. https://doi.org/10.1021/acs.analchem.5b00335
41 O. A. Alsager, S. Kumar, and J. M. Hodgkiss: Anal. Chem. **89** (2017) 7416. https://doi.org/10.1021/acs.analchem.7b0090
42 G. J. Zhang, K. S. Song, Y. Nakamura, T. Ueno, T. Funatsu, I. Ohdomori, and H. Kawarada: Langmuir **22** (2006) 3728. https://doi.org/10.1021/la050883d
43 M. Famulok and G. Mayer: Acc. Chem. Res. **44** (2011) 1349.
44 R. Nutiu and Y. Li: J. Am. Shem. Soc **18** (2003) 4771.
45 S. Ferro and A. D. Battisti: Anal. Chem. **75** (2003) 7040. https://doi.org/10.1021/ac034717r
46 R. Nutiu and Y. Li: Chem. Eur. J. **10** (2004) 1868. https://doi.org/10.1002/chem.200305470
47 M. Chandran, M. Shasha, S. Michaelson, R. Akhvlediani, and A. Hoffman: Phys. Status Solidi A **212** (2015) 2487.
48 T. Kageura, K. Kato, and H. Kawarada: Appl. Phys. Express **10** (2017) 055503. https://doi.org/10.7567/APEX.10.055503
49 E. E. Ferapontova, E. M. Olsen, and K. V. Gothelf: J. Am. Chem. Soc. **130** (2008) 4256. https://doi.org/10.1021/ja711326b
50 H. Xiao, T. E. Edwards, and A. R. Ferre-D'Amare: Chem Biol. **15** (2008) 1125. https://doi.org/10.1016/j.chembiol.2008.09.004
51 L. Kaiser, J. Weisser, M. Kohl, and H. P. Deigner: Nat. Sci. Rep. **8** (2018) 5628.